SHORT COMMUNICATION

Corticospinal excitability and conductivity are related to the anatomy of the corticospinal tract

Sonia Betti[1] · Marta Fedele[2] · Umberto Castiello[1] · Luisa Sartori[1,3] · Sanja Budisavljević[1,4]

© The Author(s), under exclusive licence to Springer-Verlag GmbH Germany, part of Springer Nature 2021

Abstract

Probing the brain structure–function relationship is at the heart of modern neuroscientific explorations, enabled by recent advances in brain mapping techniques. This study aimed to explore the anatomical blueprint of corticospinal excitability and shed light on the structure–function relationship within the human motor system. Using diffusion magnetic resonance imaging tractography, based on the spherical deconvolution approach, and transcranial magnetic stimulation (TMS), we show that anatomical inter-individual variability of the corticospinal tract (CST) modulates the corticospinal excitability and conductivity. Our findings show for the first time the relationship between increased corticospinal excitability and conductivity in individuals with a bigger CST (i.e., number of streamlines), as well as increased corticospinal microstructural organization (i.e., fractional anisotropy). These findings can have important implications for the understanding of the neuroanatomical basis of TMS as well as the study of the human motor system in both health and disease.

Introduction

The corticospinal tract (CST) is the principal motor pathway for voluntary movements and represents one of the most important descending pathways in the central nervous system. Corticospinal axons travel from the sensorimotor cortex through the internal capsule, cerebral peduncles, pons, and medulla and synapse onto the lower motor neurons of the spinal cord (Porter and Lemon 1995). A majority of axons cross the midline at the pyramidal decussation to form the lateral CST, with a small number of axons remaining on the ipsilateral side as part of the anterior CST (Nathan et al. 1990). This causes the left CST to support the voluntary movements of the right distal musculature and vice versa, a well-grounded notion in the literature. However, less is known about how the inter-individual variability in the structure of the CST affects the function of the human motor system. This study aims to explore the anatomical blueprint of corticospinal excitability and shed light on the structure–function relationship within the primary motor system.

Recent advances in neuroscientific methods have opened up new avenues for probing the relationship between structure and function. Diffusion magnetic resonance imaging (dMRI) tractography (Jones et al. 1999; Conturo et al. 1999) enables in vivo investigation of the brain's white matter connections across large samples. By following the direction of the greatest diffusivity of water molecules, one can extract orientational information and virtually reconstruct the CST (Jones 2008). This technique can be used to extract measures sensitive to either macrostructural (i.e., the number of streamlines—a proxy for volume) or microstructural properties of the CST such as myelination, axonal membrane integrity, axonal diameter, fibre density and fibre organization (i.e., fractional anisotropy—FA) (Beaulieu 2002). Best approaches combine several measures, since it is not only the presence of a connection (e.g., number of streamlines) but also the microstructural architecture (e.g., characterized

✉ Sonia Betti
    sonia.betti@unipd.it

1 Department of General Psychology, University of Padova, Padova, Italy

2 Faculty of Psychology and Educational Sciences, KU Leuven Kulak, Kortrijk, Belgium

3 Padova Neuroscience Center, University of Padova, Padova, Italy

4 School of Medicine, University of St Andrews, St Andrews, UK

by FA) that modulate conduction velocity and thus function (Seidl 2014; Mollink et al. 2019). This has been supported by studies noting a positive association between the FA and conduction velocity (Caminiti et al. 2013) or the strength of functional connectivity (van den Heuvel et al. 2008).

To probe the functional parameters of the CST, transcranial magnetic stimulation (TMS) is often used (Barker et al. 1985; Hübers et al. 2012; Rossini et al. 2015). TMS is applied to the primary motor cortex (M1) to induce cell membranes' depolarization, with action potentials travelling along the CST and peripheral motor nerves, resulting in motor-evoked potentials (MEPs) that can be recorded by surface electromyography (EMG) in contralateral muscles. TMS-induced MEPs measures, like resting motor threshold (rMT) and MEP latency, are used to derive information about the function, i.e., the corticospinal excitability and conductivity.

Previous literature suggested that the microstructural organization of the CST in terms of FA was not related to the variation in the corticospinal excitability (Herbsman et al. 2009; Hübers et al. 2012). However, to our knowledge, no study so far has used advanced dMRI tractography methods to overcome the problems of crossing fibres and partial volume effects in the M1 region, to decipher this relationship in a healthy population. Furthermore, no study has investigated whether the volumetric measures of the CST could be associated to corticospinal excitability.

Here we used advanced dMRI tractography based on the spherical deconvolution approach that successfully resolves the crossing fibres problem compared to the standard diffusion tensor model (Dell'Acqua et al. 2013). We virtually dissected the CST (M1 portion) in 19 healthy right-handed participants and assessed both volumetric (number of streamlines) and microstructural (FA) properties of this tract. Functional parameters were characterised using the TMS over M1, probing different aspects of the excitability and conduction properties of the CST (rMT, MEP amplitude, MEP latency). We hypothesized that using an advanced, more sensitive dMRI tractography approach would reveal a relationship between the structural properties of the CST, both in terms of its macro- and micro-structure, and the physiological TMS-induced MEP measures.

Materials and methods

Participants

Nineteen healthy participants (ten females), aged 23 to 33 years (mean age 27.16 ± 2.61 years), took part in the study. We determined the required sample size through the G*power software (Faul et al. 2007; bivariate normal model, two-tailed), assuming an effect size of 0.6, an alpha level of

0.05, and a power of 0.80. All subjects were healthy without a history of neurologic or psychiatric disease. All participants were right-handed with a lateralization index $> +75$ according to the Edinburgh Handedness Inventory (Oldfield 1971). The study was approved by the University of Padua Ethics Committee and carried out in accordance with the Declaration of Helsinki. Written informed consent was obtained prior to the experiment. No discomfort or other adverse effects were reported during the experiment. TMS and MRI data were acquired in two different sessions.

TMS and EMG recordings

During the TMS session (~90 min) participants were seated still in a comfortable armchair with their head kept stable by a neck pillow, their eyes open and their muscles relaxed. Single-pulse TMS (spTMS) was administered to the hand region of both left and right M1s (Fig. 1A) using a 70 mm figure-of-eight coil connected to a Magstim Bistim2 stimulator (Magstim Co., Whitland, UK). The order of the stimulation side was counterbalanced across participants. The coil was held tangentially on the scalp at a 45-degree angle to the midline (Brasil-Neto et al. 1992; Mills et al. 1992) to induce a posterior-anterior (PA) current across the central sulcus. The optimal scalp position (OSP) for the target muscle, that is the position where MEPs with maximal amplitude are recorded with minimal stimulation intensity (i.e., hand motor hotspot, hMHS), was identified by delivering single TMS pulses at fixed intensity while moving the coil of 0.5 cm around the target area until the best position was reached. The OSP was marked on a tight cap the participant wore. MEPs were acquired from the first dorsal interosseous (FDI) muscle of both left and right hands while participants were attending to a white fixation cross on black background presented in the centre of a frontal monitor. The resting motor threshold (rMT) was determined by applying ten consecutive pulses at the minimum stimulation intensity required to produce, in the relaxed contralateral FDI muscle, MEPs of more than 50 µV in the 50% of the trials (Rossini et al. 1994). Then, by increasing the intensity of stimulation to 110% of the rMT, 10 MEPs were recorded for each stimulation side to measure MEPs peak-to-peak amplitude (mV) and latency (ms; Fig. 1B). MEP latency was measured as the time elapsed between the TMS pulse and the MEP onset using the 'EMG Onset Search' algorithm implemented in the Brain Vision Analyzer software (Brain Products GmbH, Munich, Germany). This allows identifying the timepoint at which the EMG activity exceeded by more than two standard deviations the mean EMG baseline period of 100 ms recorded before the TMS pulse. The inter-pulse interval was longer than 6 s, thereby avoiding changes in corticospinal excitability due to repeated TMS pulses (Chen et al. 1997). rMT ranged from 31 to 59%

Fig. 1 TMS stimulation of left (blue) or right (violet) motor cortices and EMG recordings from FDI muscles (**A**) and a TMS-induced MEP from a representative participant, where the event-related markers in the EMG trace are used for measuring MEP latency (i.e., the time elapsed between the TMS pulse and the MEP onset – 'Lat') and peak-to-peak amplitude (i.e., the voltage difference between the maximal negative – 'Min'– and the maximal positive – 'Max'– MEP deflection) (**B**)
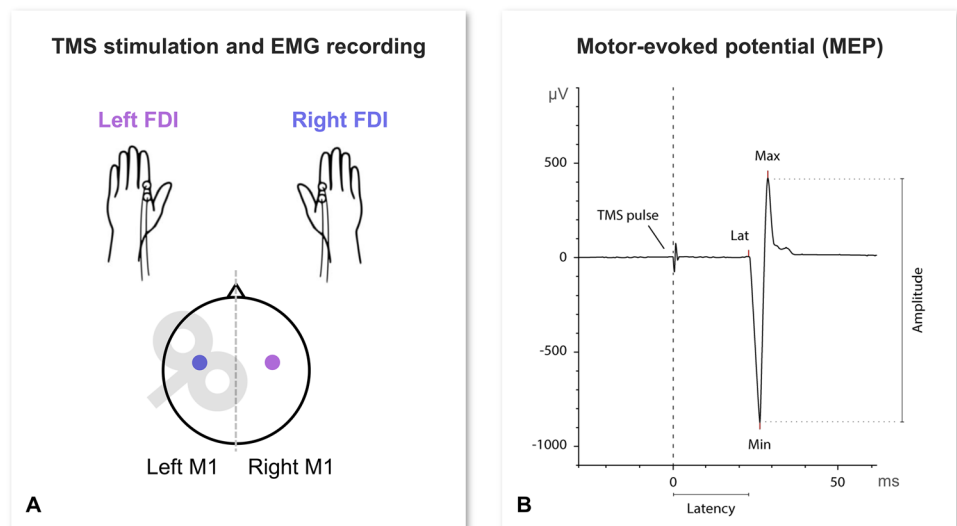
(mean = 42%, SD = 7.49) of the maximum stimulator output (MSO) for the left hemisphere and from 33 to 65% (mean = 42%, SD = 8.93) for the right hemisphere. The EMG signal was recorded (Brain Vision Recorder software, Brain Products GmbH, Munich, Germany) by means of two pairs of surface Ag/AgCl electrodes (1 cm diameter) placed in a belly-tendon montage, with the active electrode placed over the muscle belly and the reference over the interphalangeal joint (skin impedance < 5 kOhm). The ground electrode was positioned over the participant's left wrist. Electrodes were connected to an isolable portable ExG input box linked to the main EMG amplifier for signal transmission via a twin fibre optic cable (Professional BrainAmp ExG MR, Munich, Germany). The raw myographic signals were band-pass filtered (20 Hz—1 kHz), amplified prior to being digitalized (5 kHz sampling rate), and stored on a computer for off-line analysis. Trials in which any EMG activity greater than 50 µV (i.e., spike amplitude; e.g., Sartori et al. 2013) was present in the 100 ms window preceding the TMS pulse were discarded to prevent contamination of MEP measurements by background EMG activity (< 1%).

MRI data acquisition

Diffusion imaging data were acquired using a Siemens Avanto 1.5 T scanner with actively shielded magnetic field gradients (maximum amplitude 45mT/m-1) at the University Hospital of Padua. The body coil was used for RF transmission, and an 8-channel head coil for signal reception. Protocol consisted of a localizer scan, followed by a single-shot, spin-echo, EPI sequence with the following parameters: TR = 8500, TE = 97, FOV = 307.2 × 307.2, matrix size = 128 × 128, 60 slices (no gaps) with isotropic ($2.4 \times 2.4 \times 2.4$ mm^3) voxels. The maximum diffusion weighting was 2000 s/mm^2, and at each slice location 7

images were acquired with no diffusion gradients applied (b = 0 s/mm^2), together with 64 diffusion-weighted images in which gradient directions were uniformly distributed in space and repeated three times, to increase signal to noise ratio.

Correction of motion and eddy current distortion, estimation of the fibre orientation distribution and tractography algorithm

Each subject's raw image data were examined to detect for outliers in the data, including signal drop-outs, poor signal-to-noise ratio, and image artefacts such as ghosts. DWI datasets were concatenated and corrected for subject motion and geometrical distortions using ExploreDTI (http://www.exploredti.com; Leemans et al. 2009). Spherical deconvolution approach (Dell'Acqua et al. 2007) was chosen to estimate multiple orientations in voxels containing different populations of crossing fibres. It was calculated applying the damped version of the Richardson-Lucy algorithm with a fibre response parameter α = 1.5, 400 algorithm iterations and η = 0.15 and ν = 15 as threshold and geometrical regularization parameters (Dell'Acqua et al. 2010). Fibre orientation estimates were obtained by selecting the orientation corresponding to the peaks (local maxima) of the Fibre Orientation Distribution (FOD) profiles. FOD is defined as a spherical function describing for each voxel the total number of distinct fibre orientations, their actual orientations and the estimated density. To exclude spurious local maxima, we applied both an absolute and a relative threshold on the FOD amplitude (Dell'Acqua et al. 2013). The first "absolute" threshold corresponding to a Hindrance Modulated Orientational Anisotropy threshold of 0.2 was used to exclude intrinsically small local maxima due to noise or partial volume effects with isotropic tissue. The second

'relative' threshold of 5% of the maximum amplitude of the FOD was applied to remove remaining unreliable local maxima with values greater than the absolute threshold but still significantly smaller than the main fibre orientation. Whole brain tractography was performed selecting every brain voxel with at least one fibre orientation as a seed voxel. From these voxels, and for each fibre orientation, streamlines were propagated using a modified Euler integration with a step size of 0.5 mm. Streamlines were halted when a voxel without fibre orientation was reached or when the curvature between two steps exceeded a threshold of 45°. All spherical deconvolution and tractography processing were performed using StarTrack, a freely available Matlab software toolbox developed by Flavio Dell'Acqua (NatBrainLab, King's College, London).

Tractography dissections of the corticospinal tract

To visualize the CST and quantify tract-specific measures, we used TrackVis software (http://www.trackvis.org; Wang et al., 2007). We used a two regions of interest (ROIs) approach as described by Rojkova et al. (2016). The first ROI was drawn around the precentral gyrus (M1) on several consecutive axial slices where the central sulcus was clearly identifiable (Supplementary Fig. 1). The second ROI was defined around the cerebral peduncle to isolate the fibres passing from the pyramidal tract, originating from the M1 and travelling down the brainstem to the spinal cord. A "NOT" ROI was used to exclude undesired fibres passing through the ROIs but not projecting to the motor cortex. For post hoc analysis of the hand motor tract (HMT) – i.e., the section of the CST that originates from the hand motor region, the anatomical landmark of the hand motor region (omega sign) was used to delineate the first ROI on several consecutive axial slices (see Supplementary Fig. 1), with the second ROI around the cerebral peduncle being the same one used for the CST.

Data analysis

MEP peak-to-peak amplitudes and latencies (see Fig. 1B; Supplementary Table 1) were measured offline for each participant using Brain Vision Analyzer software (Brain Products GmbH, Munich, Germany). To control for the variability of MEP amplitudes, each individual's MEPs were normalized based on the largest of the ten acquired MEPs, thus scaling amplitudes values between 0 and 1 (e.g., Hübers et al. 2012). In addition to the rMT value, means of both normalized MEP amplitudes and MEP latencies were calculated separately for each participant and stimulated hemisphere. In terms of diffusion measures, the mean fractional anisotropy (FA) and the number of streamlines (NoS) of the CST were extracted.

Statistical analysis was performed using SPSS 23 software (SPSS Inc., Chicago, IL, United States). Pearson's partial correlations (r) were used to examine the relationship between the tractography variables (FA, NoS) and the MEP-related variables. We employed a false discovery rate (FDR) correction (Benjamini and Hochberg 1995) for 12 comparisons using the q-value of 0.05 for significant results (FDR $p < 0.05$), which treated for each hemisphere 2 diffusion measures (FA and NoS of the CST) and 3 TMS parameters (rMT, MEP latency and MEP amplitude) as instances of multiple testing. Only significant correlations that survived the FDR correction were reported. This FDR procedure was also employed in our post hoc analysis of the associations between TMS parameters and the hand motor tract (HMT). Furthermore, having in mind that skull-to-cortex distance (SCD) can have an effect on TMS measures (Kozel et al. 2000; McConnell et al. 2001; Stokes et al. 2005; Herbsman et al. 2009), we have measured the SCD over the left M1 and assessed its effect on our MEP-related variables using Pearson correlations. SCD was calculated from each subject's structural T1 sagittal slice, using ImageJ software (National Institutes of Health, Bethesda, MD, USA) and measuring the shortest distance (at a 90 degrees angle) from the left M1 to the skull. Where significant correlations were found, SCD was used as a control variable in partial correlations between TMS and diffusion measures. For partial correlation plots, residuals resulting from partial correlations after having controlled for SCD have been used.

Results

The effect of skull-to-cortex distance on TMS-induced measures

SCD of the left and right M1 was positively correlated with the rMT (r = 0.620, $p = 0.005$ and r = 0.684, $p = 0.001$, respectively; Fig. 2A) as well as the MEP latency (r = 0.663, $p = 0.002$ and r = 0.489, $p = 0.033$, respectively; Fig. 2B). No significant correlations emerged between SCD and the normalized MEP amplitude ($p_s > 0.05$). Hence, the SCD was used as a control variable for partial correlations with the rMT and MEP latency.

Correlations between the CST anatomy and TMS-induced measures

We found a significant negative partial correlation between the left M1 rMT and the NoS and FA of the left CST (r = − 0.620, $p = 0.006$ and r = − 0.656, $p = 0.003$, respectively; Fig. 3). No significant correlations emerged between the left CST measures and MEP latency ($p_s > 0.05$; Suppl. Table 2). A significant negative correlation was found

Fig. 2 Correlations between SCD and rMT (**A**) and MEP latency (**B**) for the left (blue circles) and right (violet squares) hemispheres
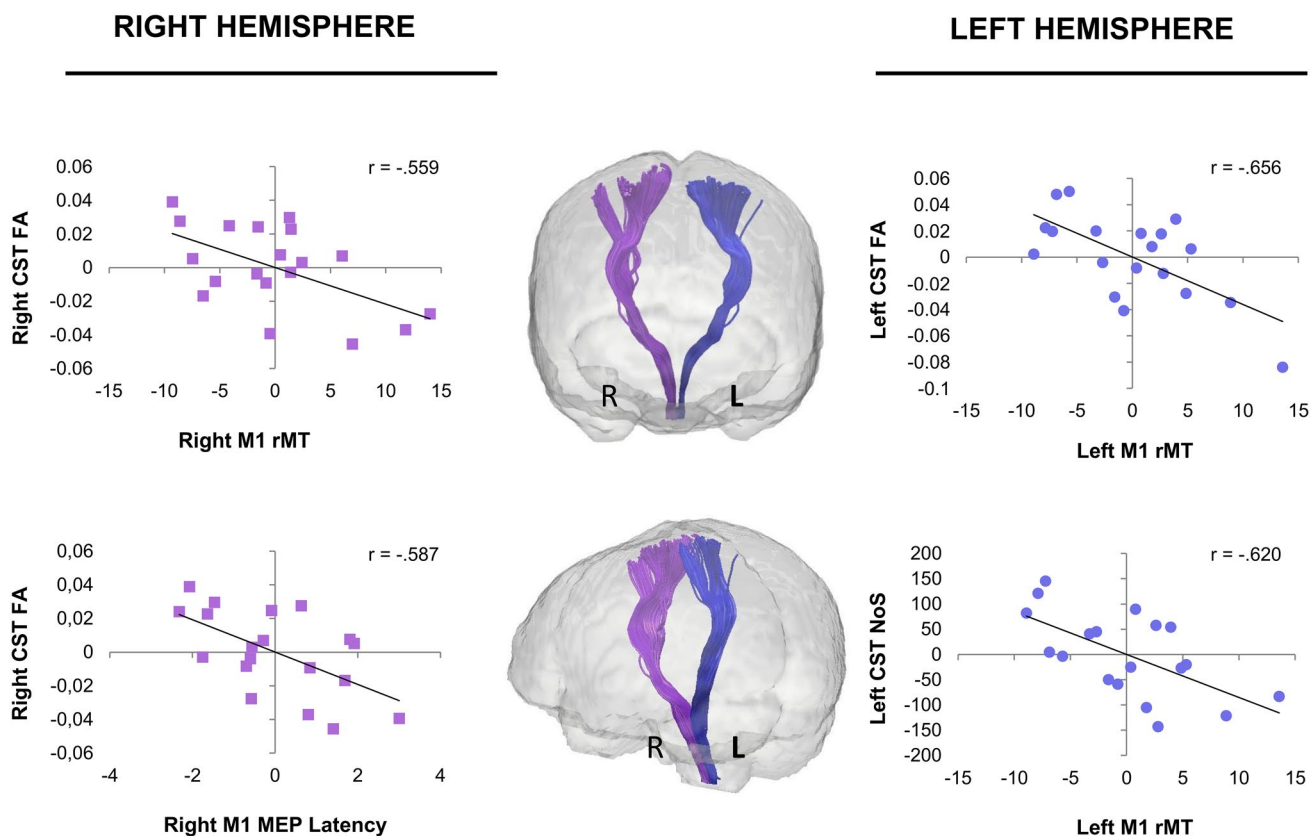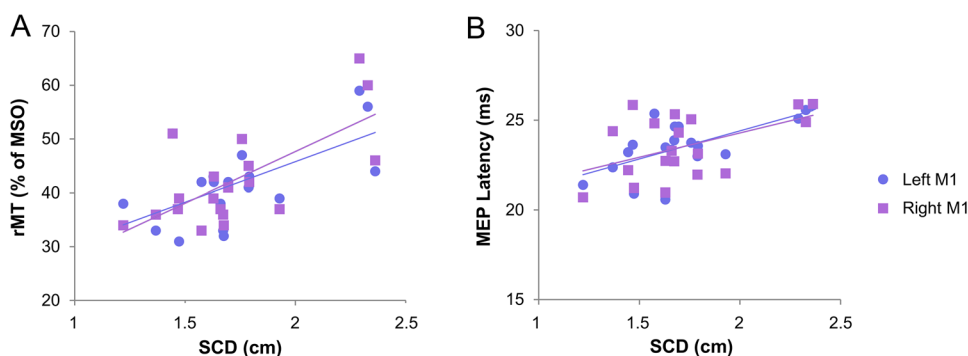

Fig. 3 Significant partial correlations between the structure of the CST (FA or NoS residuals) and the TMS-induced measures (rMT or MEP latency residuals) in the right (violet) and left (blue) hemispheres

between the FA of the right CST and the right M1 rMT ($r = -0.559$, $p = 0.016$; Fig. 3) as well as the right MEP latency ($r = -0.587$, $p = 0.011$; Fig. 3). For the MEP amplitude at 110% of the rMT, no significant correlations were found with the CST structural measures ($p_s > 0.05$; Suppl. Table 2).

Lastly, we have performed a post hoc analysis of the hand motor tract (HMT), as a section of the CST that originates from the hand motor area. We have replicated the negative association between the FA and the rMT for the left hemisphere ($r = -0.515$, $p = 0.029$), but it failed to survive the FDR correction. No other significant correlations emerged ($p_s > 0.066$). However, it should be taken into account that the HMT ROI was anatomically defined, and thus lacks the sensitivity and specificity of a functionally defined ROI in light of a significant inter-individual variability in the location of the hand motor region (e.g., Sun et al. 2012; Eichert et al. 2021).

Discussion

This is the first study in a healthy population that used advanced dMRI tractography and TMS to show that the anatomy of the CST modulates the corticospinal excitability and conductivity. The higher FA of the bilateral CST corresponded to a higher corticospinal excitability as indexed by rMT, whereas higher FA of the right CST corresponded to lower MEP latency or, in other words, faster conductivity. Furthermore, this is the first study that investigated how the inter-individual variability in the volumetric properties of the CST modulates the corticospinal excitability. We found that corticospinal excitability is increased in individuals with a higher number of CST streamlines in the dominant (left) hemisphere. Our findings shed light on the neurophysiological correlates of the inter-individual variability of the CST and show that the facilitation of the corticospinal excitability in the ipsilateral M1 is associated with the macro- and micro-structural variation of the corticospinal descending pathway.

The observed inter-individual variation in the structure of the CST could be driven by genetic, epigenetic or environmental factors. Variation in experience that may induce structural changes in the CST is especially relevant having in mind that this tract continues to mature well into the second decade of life (Dubois et al. 2009). CST developmental profile is similar to the one of M1, which is considered to be a dynamic motor control region exhibiting activity-dependent plasticity (Sanes and Donoghue 2000).

To study the neurophysiological correlates of the CST we have used a TMS technique, a well-established tool for studying the excitability and conductivity of fast monosynaptic corticospinal projections originating in M1. A single suprathreshold TMS pulse on the CST, as assessed by epidural invasive recordings at the level of the cervical spinal cord, gives rise to a series of descending volleys, namely direct (D-) and indirect (I-) waves in the corticospinal pathway (for a review, see Di Lazzaro and Rothwell 2014), generated by fast conducting corticospinal neurons connected monosynaptically with spinal motoneurons (Groppa et al. 2012). Following primary motor cortex stimulation, MEPs are elicited in peripheral muscles and their latency and amplitude can be estimated. The rMT, which is an indicator of the level of corticospinal excitability, shows inter-individual variability and varies across muscles, with lower thresholds for hand and forearm muscles than truncal, limb and pelvic musculature (Tranulis et al. 2006; Rossini et al. 2015). Importantly, the rMT reflects membrane excitability and local density of individual neurons (Hallett 2000), but also excitability at the level of cortico-cortical axons and their excitatory synaptic connections with corticospinal neurons (Farzan

2014). This means that the rMT reflects membrane excitability both at the level of corticospinal axons in the motor cortex, as well as at the levels of motor neurons in the spinal cord, neuromuscular junction and muscle (Kobayashi and Pascual-Leone 2003). rMT is often altered (increased) in diseases affecting the corticospinal tract, such as brain and spinal cord injury, multiple sclerosis or stroke (for reviews see Groppa et al. 2012; Rossini et al. 2015). This study showed that the rMT, as an index of corticospinal excitability, is associated with the FA of the CST bilaterally, and with the CST number of streamlines in the left hemisphere only. This leftward asymmetry of volumetric results should be replicated in larger samples. No significant results emerged when considering MEPs amplitude acquired by stimulating M1 at 110% of rMT. This could be related to the fact that motor threshold and MEP amplitude reflect different physiological mechanisms, as suggested by the differential effects on these measures induced by drugs acting on neurotransmitters or on modulators of neurotransmission (Ziemann 2004). In addition, by adopting an above-threshold stimulation, we calibrated and normalized the TMS stimulation controlling for individual structural (e.g., SCD) and physiologic variability. Therefore, rMT appears to be a better candidate to investigate the relationship between TMS physiology and its corresponding white matter correlates. Our findings suggest that increased fibre organization, axonal membrane integrity, myelination or axon diameter of the bilateral CST (indexed by higher FA) could lead to higher corticospinal excitability and conductivity.

This is in line with studies showing that electrical conductivity and anisotropic diffusion are closely related (Tuch et al. 2001; Haueisen et al. 2002) since the same geometric tissue properties lead to an increase in both anisotropy and conductivity. However, our findings are contrary to previous research that failed to find a clear link between the CST microstructure (indexed by FA) and the variation in the corticospinal excitability. Nevertheless, the fibre-tracking algorithm of diffusion tensor model often used in previous studies could not resolve the problem of crossing white matter bundles. This could lead to incomplete tracking of the M1 portion of the CST, stemming from the rich density of fibres crossings in the area.

It should be noted that the majority of studies failed to delineate the entire CST with tractography (e.g., Herbsman et al. 2009) and used approaches that focused only on specific CST parts or voxels such as tract-based spatial statistics (TBSS) or voxel-based analysis (Hübers et al. 2012). Our approach, instead, was more sensitive to discern the association since the spherical deconvolution approach accurately resolves crossing fibres even in noisy data and preserves the angular resolution of the main fibre orientations in the presence of partial volume contamination (Dell'Acqua et al.

2013). Thus, we could observe strong associations between several structural and functional measures of the corticospinal motor system. The findings that corticospinal excitability increased with higher white matter FA is in line with previous studies observing the same direction of association, though in regions generally outside the CST (Klöppel et al. 2008) or connected to M1 (i.e., the dorsal premotor cortex; Rosso et al. 2017). However, it should be mentioned that the corticospinal tract can be best investigated only using neural tracers in non-human primates and directly watching the labeling within the spinal sectors. With dMRI tractography it is difficult to disentangle the corticofugal from the corticospinal fibres, and this should be taken into account when interpreting the findings.

Differently from the rMT, latency measures the time that passes from the delivery of a single TMS pulse and the appearance of the MEP in the EMG response of a target muscle. As for the rMT, latency varies across muscles, being shorter for the upper extremities muscles than for the low extremities ones, being also influenced by height especially in the lower limbs (Tobimatsu et al. 1998; Farzan 2014; Cantone et al. 2019). MEP latency reflects the number of synapses between the stimulation site and the peripheral muscle, being influenced by the diameter and the myelin sheath thickness of the crossed fibres (Farzan 2014). These microstructural properties are reflected in the dMRI derived measure of FA, and our results support the notion that higher axonal membrane integrity, myelination or axon diameter of the right CST (higher FA) correspond to faster conduction time, i.e., lower MEP latency. Dubbioso et al. (2021) recently attempted to investigate the relationship between structure and function in the motor hand knob by combining myelin-sensitive MRI, functional MRI during the execution of a motor task, as well as MEP recording. They demonstrated that a higher degree of myelination in the precentral motor hand knob was associated with more rostral TMS hotspots, suggesting that inter-individual differences in precentral myelination could account for variations in corticospinal excitability, as well as in dexterous motor control (Dubbioso et al. 2021). According to this innovative approach, our results showing an asymmetric relationship between structural CST measures and MEP latency (i.e., a positive correlation only for right FA and MEP latency) could be associated to differences in the hotspot rostrality (see also Ahdab et al. 2016) and should be replicated in bigger samples.

Along this line, some studies also reported a non-complete overlap between the hMHS and the hand knob (Ahdab et al. 2016; Kim et al. 2021). In our post hoc analysis focused on the on the section of the CST that originates from the hand motor region (based on the omega sign, an anatomical landmark), as compared to the CST fibers originating from the whole M1, the correlations between the tractography and the MEP-related variables were less strong and only partially overlapping. This points to the possible effect of anatomical variability in the hMHS location among individuals – which may not coincide with the anatomically defined hand knob as shown by Kim et al. (2021). This could affect the sensibility of our results and the lack of observed associations.

Along with the rMT, future studies should also probe the strength of corticospinal projections through the input/output (I/O) curve or recruitment curve, thus measuring the modulation of MEP amplitudes across a wide range of TMS intensities (Devanne et al. 1997). As temporospatial summation at the cortico-motorneuronal synapses is enhanced by increasing stimulus intensity, the slope and the plateau phase of the I/O curve will reflect the number of recruited corticospinal fibres and the temporal dispersion of the descending excitatory drive along the corticomotor pathways (Rossini et al. 2015). In the present study, we did not find any significant correlation between CST structural features and MEP amplitudes. However, a limitation is having measured amplitudes by recording ten MEPs. Although it could be sufficient for obtaining a reliable measure of CSE (e.g., Bastani and Jaberzadeh 2012; Cavaleri et al. 2017), an increase in the number of acquired MEPs (e.g., 20–30; Cuypers et al. 2014; Goldsworthy et al. 2016; see also Ammann et al. 2020) would surely have improved the reliability of the obtained results given the well-known trial-to-trial intrinsic variability in MEP amplitudes.

In summary, as TMS can evoke neuronal activity by exciting neurons in a suprathreshold fashion, it is well suited to investigate excitability and connectivity in targeted areas (Siebner et al. 2009), giving researchers the chance to shed light on the structural substrates of observed TMS effects and measures that are still poorly understood (Bestmann and Krakauer 2015). Along this line, neuroimaging in conjunction with TMS can be used to advance the understanding of the TMS technique itself (Bergmann et al. 2016). Future research should further expand our knowledge on the CST structure–function relation, which may positively affect the diagnostic and therapeutic potential of TMS combined with dMRI measures in various neurological and psychiatric disorders, as well as traumas causing structural and functional changes (e.g., Du et al. 2017; Jang et al. 2017; Zhao et al. 2019; Jang and Seo 2019; Guder et al. 2020, 2021; Mirchandani et al. 2020). In addition, future studies exploring the corticospinal tract should apply a field map correction that could affect the cerebral peduncles where the second ROI is placed. Even if our sample size is in line with previous literature (e.g., Hübers et al. 2012), our findings could benefit from a replication in larger samples, this way providing an even more reliable reference for the structure–function relationship in healthy individuals.

In conclusion, by coupling neurophysiology with neuroanatomy, our study has shown that both macro- and

microstructural properties of the CST are associated with the corticospinal excitability and conductivity. Our results shed important light onto the structure–function relationship of the human motor system relevant for both health and disease.

Supplementary Information The online version contains supplementary material available at https://doi.org/10.1007/s00429-021-02410-9.

Availability of data and material The datasets generated and analysed during the current study are available from the corresponding author on reasonable request.

Declarations

Conflicts of interest The authors declare that they have no conflict of interest.

Ethics approval All procedures performed in studies involving human participants were in accordance with the ethical standards of the Ethics Committee of the University of Padova, Italy, and with the 1964 Helsinki Declaration and its later amendments or comparable ethical standards.

Consent to participate Written informed consent was obtained from all participants included in the study.

References

Ahdab R, Ayache SS, Brugières P et al (2016) The hand motor hotspot is not always located in the hand knob: a neuronavigated transcranial magnetic stimulation study. Brain Topogr 29:590–597. https://doi.org/10.1007/s10548-016-0486-2

Ammann C, Guida P, Caballero-Insaurriaga J et al (2020) A framework to assess the impact of number of trials on the amplitude of motor evoked potentials. Sci Rep 10:21422. https://doi.org/10.1038/s41598-020-77383-6

Barker AT, Jalinous R, Freeston IL (1985) Non-invasive magnetic stimulation of human motor cortex. The Lancet 325:1106–1107. https://doi.org/10.1016/S0140-6736(85)92413-4

Bastani A, Jaberzadeh S (2012) A higher number of TMS-elicited MEP from a combined hotspot improves intra- and inter-session reliability of the upper limb muscles in healthy individuals. PLoS ONE 7:e47582. https://doi.org/10.1371/journal.pone.0047582

Beaulieu C (2002) The basis of anisotropic water diffusion in the nervous system – a technical review. NMR Biomed 15:435–455. https://doi.org/10.1002/nbm.782

Benjamini Y, Hochberg Y (1995) Controlling the False Discovery Rate: A Practical and Powerful Approach to Multiple Testing. J R Stat Soc Ser B Methodol 57:289–300. https://doi.org/10.1111/j.2517-6161.1995.tb02031.x

Bergmann TO, Karabanov A, Hartwigsen G et al (2016) Combining non-invasive transcranial brain stimulation with neuroimaging and electrophysiology: Current approaches and future perspectives. Neuroimage 140:4–19. https://doi.org/10.1016/j.neuroimage.2016.02.012

Bestmann S, Krakauer JW (2015) The uses and interpretations of the motor-evoked potential for understanding behaviour. Exp Brain Res 233:679–689. https://doi.org/10.1007/s00221-014-4183-7

Brasil-Neto JP, Cohen LG, Panizza M et al (1992) Optimal focal transcranial magnetic activation of the human motor cortex: effects of coil orientation, shape of the induced current pulse, and stimulus intensity. J Clin Neurophysiol 9:132

Caminiti R, Carducci F, Piervincenzi C et al (2013) Diameter, length, speed, and conduction delay of callosal axons in macaque monkeys and humans: comparing data from histology and magnetic resonance imaging diffusion tractography. J Neurosci 33:14501–14511. https://doi.org/10.1523/JNEUROSCI.0761-13.2013

Cantone M, Lanza G, Vinciguerra L et al (2019) Age, height, and sex on motor evoked potentials: translational data from a large italian cohort in a clinical environment. Front Hum Neurosci 13:185. https://doi.org/10.3389/fnhum.2019.00185

Cavaleri R, Schabrun SM, Chipchase LS (2017) The number of stimuli required to reliably assess corticomotor excitability and primary motor cortical representations using transcranial magnetic stimulation (TMS): a systematic review and meta-analysis. Syst Rev 6:48. https://doi.org/10.1186/s13643-017-0440-8

Chen R, Gerloff C, Classen J et al (1997) Safety of different inter-train intervals for repetitive transcranial magnetic stimulation and recommendations for safe ranges of stimulation parameters. Electroencephalogr Clin Neurophysiol Mot Control 105:415–421. https://doi.org/10.1016/S0924-980X(97)00036-2

Conturo TE, Lori NF, Cull TS et al (1999) Tracking neuronal fiber pathways in the living human brain. Proc Natl Acad Sci 96:10422–10427. https://doi.org/10.1073/pnas.96.18.10422

Cuypers K, Thijs H, Meesen RLJ (2014) Optimization of the transcranial magnetic stimulation protocol by defining a reliable estimate for corticospinal excitability. PLoS ONE 9:e86380. https://doi.org/10.1371/journal.pone.0086380

Dell'Acqua F, Rizzo G, Scifo P et al (2007) A Model-based deconvolution approach to solve fiber crossing in diffusion-weighted MR imaging. IEEE Trans Biomed Eng 54:462–472. https://doi.org/10.1109/TBME.2006.888830

Dell'Acqua F, Scifo P, Rizzo G et al (2010) A modified damped Richardson-Lucy algorithm to reduce isotropic background effects in spherical deconvolution. Neuroimage 49:1446–1458. https://doi.org/10.1016/j.neuroimage.2009.09.033

Dell'Acqua F, Simmons A, Williams SCR, Catani M (2013) Can spherical deconvolution provide more information than fiber orientations? Hindrance modulated orientational anisotropy, a true-tract specific index to characterize white matter diffusion. Hum Brain Mapp 34:2464–2483. https://doi.org/10.1002/hbm.22080

Devanne H, Lavoie BA, Capaday C (1997) Input-output properties and gain changes in the human corticospinal pathway. Exp Brain Res 114:329–338. https://doi.org/10.1007/pl00005641

Di Lazzaro V, Rothwell JC (2014) Corticospinal activity evoked and modulated by non-invasive stimulation of the intact human motor cortex. J Physiol 592:4115–4128. https://doi.org/10.1113/jphysiol.2014.274316

Du X, Kochunov P, Summerfelt A et al (2017) The role of white matter microstructure in inhibitory deficits in patients with schizophrenia. Brain Stimulat 10:283–290. https://doi.org/10.1016/j.brs.2016.11.006

Dubbioso R, Madsen KH, Thielscher A, Siebner HR (2021) The myelin content of the human precentral hand knob reflects interindividual differences in manual motor control at the physiological and behavioral level. J Neurosci 41:3163–3179. https://doi.org/10.1523/JNEUROSCI.0390-20.2021

Dubois J, Hertz-Pannier L, Cachia A et al (2009) Structural asymmetries in the infant language and sensori-motor networks. Cereb Cortex 19:414–423. https://doi.org/10.1093/cercor/bhn097

Eichert N, Watkins KE, Mars RB, Petrides M (2021) Morphological and functional variability in central and subcentral motor cortex of the human brain. Brain Struct Funct 226:263–279. https://doi.org/10.1007/s00429-020-02180-w

Farzan F (2014) Single-pulse transcranial magnetic stimulation (TMS) protocols and outcome measures. In: Rotenberg A, Horvath JC, Pascual-Leone A (eds) Transcranial magnetic stimulation. Springer, New York, NY, pp 69–115

Faul F, Erdfelder E, Lang A-G, Buchner A (2007) G*Power 3: A flexible statistical power analysis program for the social, behavioral, and biomedical sciences. Behav Res Methods 39:175–191. https://doi.org/10.3758/BF03193146

Goldsworthy MR, Hordacre B, Ridding MC (2016) Minimum number of trials required for within- and between-session reliability of TMS measures of corticospinal excitability. Neuroscience 320:205–209. https://doi.org/10.1016/j.neuroscience.2016.02.012

Groppa S, Oliviero A, Eisen A et al (2012) A practical guide to diagnostic transcranial magnetic stimulation: Report of an IFCN committee. Clin Neurophysiol 123:858–882. https://doi.org/10.1016/j.clinph.2012.01.010

Guder S, Frey BM, Backhaus W et al (2020) The influence of cortico-cerebellar structural connectivity on cortical excitability in chronic stroke. Cereb Cortex 30:1330–1344. https://doi.org/10.1093/cercor/bhz169

Guder S, Pasternak O, Gerloff C, Schulz R (2021) Strengthened structure–function relationships of the corticospinal tract by free water correction after stroke. Brain Commun. https://doi.org/10.1093/braincomms/fcab034

Hallett M (2000) Transcranial magnetic stimulation and the human brain. Nature 406:147–150. https://doi.org/10.1038/35018000

Haueisen J, Tuch DS, Ramon C et al (2002) The Influence of Brain Tissue Anisotropy on Human EEG and MEG. Neuroimage 15:159–166. https://doi.org/10.1006/nimg.2001.0962

Herbsman T, Forster N, Molnar C et al (2009) Motor threshold in transcranial magnetic stimulation: The impact of white matter fiber orientation and skull-to-cortex distance. Hum Brain Mapp 30:2044–2055. https://doi.org/10.1002/hbm.20649

Hübers A, Klein JC, Kang J-S et al (2012) The relationship between TMS measures of functional properties and DTI measures of microstructure of the corticospinal tract. Brain Stimulat 5:297–304. https://doi.org/10.1016/j.brs.2011.03.008

Jang SH, Seo YS (2019) Diagnosis of conversion disorder using diffusion tensor tractography and transcranial magnetic stimulation in a patient with mild traumatic brain injury. Diagnostics 9:155. https://doi.org/10.3390/diagnostics9040155

Jang SH, Kim DH, Kim SH, Seo JP (2017) The relation between the motor evoked potential and diffusion tensor tractography for the corticospinal tract in chronic hemiparetic patients with cerebral infarct. Somatosens Mot Res 34:134–138. https://doi.org/10.1080/08990220.2017.1343188

Jones DK (2008) Studying connections in the living human brain with diffusion MRI. Cortex 44:936–952. https://doi.org/10.1016/j.cortex.2008.05.002

Jones DK, Simmons A, Williams SCR, Horsfield MA (1999) Non-invasive assessment of axonal fiber connectivity in the human brain via diffusion tensor MRI. Magn Reson Med 42:37–41. https://doi.org/10.1002/(SICI)1522-2594(199907)42:1%3c37::AID-MRM7%3e3.0.CO;2-O

Kim H, Kim J, Lee H-J, et al (2021) Optimal stimulation site for rTMS to improve motor function: Anatomical hand knob vs. hand motor hotspot. Neurosci Lett 740:135424. https://doi.org/10.1016/j.neulet.2020.135424

Klöppel S, Bäumer T, Kroeger J et al (2008) The cortical motor threshold reflects microstructural properties of cerebral white matter. Neuroimage 40:1782–1791. https://doi.org/10.1016/j.neuroimage.2008.01.019

Kobayashi M, Pascual-Leone A (2003) Transcranial magnetic stimulation in neurology. Lancet Neurol 2:145–156. https://doi.org/10.1016/S1474-4422(03)00321-1

Kozel FA, Nahas Z, deBrux C et al (2000) How coil-cortex distance relates to age, motor threshold, and antidepressant response to repetitive transcranial magnetic stimulation. J Neuropsychiatry Clin Neurosci 12:376–384. https://doi.org/10.1176/jnp.12.3.376

Leemans A, Jeurissen B, Sijbers J, Jones DK (2009) ExploreDTI: a graphical toolbox for processing, analyzing, and visualizing diffusion MR data. Hawaii, USA, p 3537

McConnell KA, Nahas Z, Shastri A et al (2001) The transcranial magnetic stimulation motor threshold depends on the distance from coil to underlying cortex: a replication in healthy adults comparing two methods of assessing the distance to cortex. Biol Psychiatry 49:454–459. https://doi.org/10.1016/S0006-3223(00)01039-8

Mills KR, Boniface SJ, Schubert M (1992) Magnetic brain stimulation with a double coil: the importance of coil orientation. Electroencephalogr Clin Neurophysiol Potentials Sect 85:17–21. https://doi.org/10.1016/0168-5597(92)90096-T

Mirchandani AS, Beyh A, Lavrador JP et al (2020) Altered corticospinal microstructure and motor cortex excitability in gliomas: an advanced tractography and transcranial magnetic stimulation study. J Neurosurg 1:1–9. https://doi.org/10.3171/2020.2.JNS192994

Mollink J, Smith SM, Elliott LT et al (2019) The spatial correspondence and genetic influence of interhemispheric connectivity with white matter microstructure. Nat Neurosci 22:809–819. https://doi.org/10.1038/s41593-019-0379-2

Nathan PW, Smith MC, Deacon P (1990) The corticospinal tracts in man: Course and location of fibres at different segmental levels. Brain 113:303–324. https://doi.org/10.1093/brain/113.2.303

Oldfield RC (1971) The assessment and analysis of handedness: The Edinburgh inventory. Neuropsychologia 9:97–113. https://doi.org/10.1016/0028-3932(71)90067-4

Porter R, Lemon R (1995) Corticospinal function and voluntary movement. Oxford University Press

Rojkova K, Volle E, Urbanski M et al (2016) Atlasing the frontal lobe connections and their variability due to age and education: a spherical deconvolution tractography study. Brain Struct Funct 221:1751–1766. https://doi.org/10.1007/s00429-015-1001-3

Rossini PM, Barker AT, Berardelli A et al (1994) Non-invasive electrical and magnetic stimulation of the brain, spinal cord and roots: basic principles and procedures for routine clinical application. Report of an IFCN committee. Electroencephalogr Clin Neurophysiol 91:79–92. https://doi.org/10.1016/0013-4694(94)90029-9

Rossini PM, Burke D, Chen R et al (2015) Non-invasive electrical and magnetic stimulation of the brain, spinal cord, roots and peripheral nerves: Basic principles and procedures for routine clinical and research application. An updated report from an I.F.C.N. Committee Clin Neurophysiol 126:1071–1107. https://doi.org/10.1016/j.clinph.2015.02.001

Rosso C, Perlbarg V, Valabregue R et al (2017) Anatomical and functional correlates of cortical motor threshold of the dominant hand. Brain Stimulat 10:952–958. https://doi.org/10.1016/j.brs.2017.05.005

Sanes JN, Donoghue JP (2000) Plasticity and Primary Motor Cortex. Annu Rev Neurosci 23:393–415. https://doi.org/10.1146/annurev.neuro.23.1.393

Sartori L, Betti S, Castiello U (2013) Corticospinal excitability modulation during action observation. J vis Exp JoVE. https://doi.org/10.3791/51001

Seidl AH (2014) Regulation of conduction time along axons. Neuroscience 276:126–134. https://doi.org/10.1016/j.neuroscience.2013.06.047

Siebner HR, Hartwigsen G, Kassuba T, Rothwell JC (2009) How does transcranial magnetic stimulation modify neuronal activity in the

brain? Implications for studies of cognition. Cortex 45:1035–1042. https://doi.org/10.1016/j.cortex.2009.02.007

Stokes MG, Chambers CD, Gould IC et al (2005) Simple metric for scaling motor threshold based on scalp-cortex distance: application to studies using transcranial magnetic stimulation. J Neurophysiol 94:4520–4527. https://doi.org/10.1152/jn.00067.2005

Sun ZY, Klöppel S, Rivière D et al (2012) The effect of handedness on the shape of the central sulcus. Neuroimage 60:332–339. https://doi.org/10.1016/j.neuroimage.2011.12.050

Tobimatsu S, Sun S-J, Fukui R, Kato M (1998) Effects of sex, height and age on motor evoked potentials with magnetic stimulation. J Neurol 245:256–261. https://doi.org/10.1007/s004150050215

Tranulis C, Guéguen B, Pham-Scottez A et al (2006) Motor threshold in transcranial magnetic stimulation: comparison of three estimation methods. Neurophysiol Clin Neurophysiol 36:1–7. https://doi.org/10.1016/j.neucli.2006.01.005

Tuch DS, Wedeen VJ, Dale AM et al (2001) Conductivity tensor mapping of the human brain using diffusion tensor MRI. Proc Natl Acad Sci 98:11697–11701. https://doi.org/10.1073/pnas.171473898

van den Heuvel MP, Stam CJ, Boersma M, Hulshoff Pol HE (2008) Small-world and scale-free organization of voxel-based resting-state functional connectivity in the human brain. Neuroimage 43:528–539. https://doi.org/10.1016/j.neuroimage.2008.08.010

Zhao EY, Vavasour IM, Zakeri M et al (2019) Myelin water imaging and transcranial magnetic stimulation suggest structure-function relationships in multiple sclerosis. Front Phys. https://doi.org/10.3389/fphy.2019.00141

Ziemann U (2004) TMS and drugs. Clin Neurophysiol 115:1717–1729. https://doi.org/10.1016/j.clinph.2004.03.006